nature reviews earth & environment

https://doi.org/10.1038/s43017-024-00638-7

Review article

Check for updates

Atmospheric rivers in Antarctica

Jonathan D. Wille[1,26] ✉, Vincent Favier[2,26], Irina V. Gorodetskaya[3,26], Cécile Agosta[4], Rebecca Baiman[5], J. E. Barrett[6], Léonard Barthelemy[7], Burcu Boza[8], Deniz Bozkurt[9,10,11], Mathieu Casado[4], Anastasiia Chyhareva[12,13], Kyle R. Clem[14], Francis Codron[7], Rajashree Tri Datta[15], Claudio Durán-Alarcón[3], Diana Francis[16], Andrew O. Hoffman[17], Marlen Kolbe[18], Svitlana Krakovska[12,13], Gabrielle Linscott[19], Michelle L. Maclennan[5], Kyle S. Mattingly[20], Ye Mu[21], Benjamin Pohl[22], Christophe Leroy-Dos Santos[4], Christine A. Shields[23], Emir Toker[8], Andrew C. Winters[5], Ziqi Yin[5], Xun Zou[24], Chen Zhang[25] & Zhenhai Zhang[24]

Abstract

Antarctic atmospheric rivers (ARs) are a form of extreme weather that transport heat and moisture from the Southern Hemisphere subtropics and/or mid-latitudes to the Antarctic continent. Present-day AR events generally have a positive influence on the Antarctic ice-sheet mass balance by producing heavy snowfall, yet they also cause melt of sea ice and coastal ice sheet areas, as well as ice shelf destabilization. In this Review, we explore the atmospheric dynamics and impacts of Antarctic ARs over their life cycle to better understand their net contributions to ice-sheet mass balance. ARs occur in high-amplitude pressure couplets, and those strong enough to reach the Antarctic are often formed within Rossby waves initiated by tropical convection. Antarctic ARs are rare events (~3 days per year per location) but have been responsible for 50–70% of extreme snowfall events in East Antarctica since the 1980s. However, they can also trigger extensive surface melting events, such as the final ice shelf collapse of Larsen A in 1995 and Larsen B in 2002. Climate change will likely cause stronger ARs as anthropogenic warming increases atmospheric water vapour. Future research must determine how these climate change impacts will alter the relationship among Antarctic ARs, net ice-sheet mass balance and future sea-level rise.

Sections

A full list of affiliations appears at the end of the paper. ✉e-mail: jonathan.wille@env.ethz.ch

Introduction

Atmospheric rivers (ARs) are a major component of the global water cycle. They form in the middle and subtropical latitudes and redistribute vast amounts of moisture (up to 250,000 m^3 per AR) around the globe in the form of long (>2,000 km), narrow (<1,000 km) bands that travel through the troposphere (Fig. 1). ARs that reach mid-latitude continents are typically associated with extreme precipitation events, such as drought-busting and/or flooding rainfall[1]. However, ARs can also travel all the way to the high latitudes, and their moisture provides the majority (up to 90% depending on the AR detection method) of water vapour transport to polar regions[2,3]. In Antarctica, the world's largest desert, extreme precipitation events control the water supply[4]. ARs have been responsible for 50–70% of extreme snowfall events in East Antarctica since the 1980s, therefore directly contributing to the mass balance of the Antarctic ice sheet (AIS). As Antarctica has the largest mass of ice on Earth, representing a sea-level equivalent of 58 m and 70% of global fresh water[5,6], understanding the behaviour of Antarctic ARs and their impacts on ice sheets is crucial for constraining global sea-level rise projections. Especially, it will be imperative to understand how ARs and their impacts will be effected by climate change as extreme weather becomes increasingly common[4].

Only some ARs manage to travel over the many thousand kilometres across the Southern Ocean until they reach the Antarctic coastline[7]. Certain interactions between lower and mid-latitude atmospheric dynamics enable ARs to propagate over these vast distances, including tropical thunderstorms and cyclones, the mid-latitude jet stream and storms and their influence on high-latitude stationary high-pressure systems (blocks)[7–9]. If an AR reaches Antarctica or the surrounding sea ice regions, the warm and moist air within the AR interacts with the cold and dry air above the surface, leading to mixed weather impacts along the seasonal sea ice pack and coastline, whereby they are termed Antarctic ARs. The moisture precipitates out as snowfall and/or rainfall, whereas the warm air can cause extensive surface melting and sea ice disintegration[7,10,11]. These interactions make Antarctic ARs unique compared with mid-latitude ARs.

Since the first connection between ARs and several anomalous snowfall events in East Antarctica in 2009 and 2011 was established[12,13], measurements and observations of ARs have extended to the AIS and Southern Ocean and are showing a multitude of mass-balance impacts. For example, some ARs have been shown to create contrasting mass balance impacts to the AIS and include the majority of extreme snowfall events, major surface melt, anomalous rainfall, ice shelf instability, sea ice disintegration and polynya formation[7,10,14–16]. The full spectrum of AR impacts was particularly highlighted in 2022 by a major AR that reached the Antarctic coast. The snowfall from this event helped to make 2022 a positive mass balance year for the AIS (uncommon in the past 20 years)[17,18], but it also pushed the final collapse of the Conger ice shelf while triggering rare autumn surface melt along the East Antarctica coastline[14]. Current and future Antarctic snow storage and its contribution to sea-level rise will thus be strongly influenced by ARs.

In this Review, we provide an overview of Antarctic AR dynamics, climatology and impacts on the health of the AIS. We discuss the typical life cycle of an Antarctic-specific AR, including the hemispheric scale, synoptic-scale, mesoscale and microphysical dynamics. Specially adapted detection and measurement techniques are necessary for studying ARs in the cold and dry environment of Antarctica. We explore the historical and future trends of AR frequency and interannual variability and discuss their impacts on the AIS. Future research should focus on how AR impacts will evolve in the future with climate change.

Antarctic AR dynamics

Through varying levels of spatial scales, Antarctic ARs have distinctive dynamical characteristics from their origin points to their eventual landfall. In this section, we present the typical AR life cycle across the large global scale, synoptic scale and mesoscale, along with their characteristic cloud water (or aerosol) content and microphysics.

Global-scale dynamics

Antarctic ARs occur in regions of strong poleward flow between a synoptic (spanning 1,000–2,500 km) cyclone (to the west) and a ridge of high pressure (to the east). They become embedded in a mid-tropospheric wave pattern over the Southern Hemisphere mid-latitudes and adjacent Southern Ocean[8,9,19] (Fig. 1). AR landfalls are primarily driven by meridional moisture transport, except over the Antarctic Peninsula (AP) where there can also be a strong zonal advective component[20]. This zonal advection of moisture is partly influenced by the phase polarity of the Southern Annual Mode (the intensity and latitudinal positioning of the belt of strong westerly winds surrounding Antarctica), which can be seen as the degree of coupling between the Antarctic continent and the southern hemisphere mid-latitudes[21].

Antarctic ARs are often embedded within an extratropical high–low pressure couplet. An amplified mid-tropospheric wave pattern, such as zonal wavenumber 3 (ref. 22), can provide favourable background conditions for AR formation. Strong ARs (for example, those transporting the highest amounts of moisture, 300–1,000 kg m^{-1} s^{-2}, or causing the heaviest precipitation over land, >0.5 Gt h^{-1})[9,14,23] tend to occur when the extratropical flow pattern becomes coupled with a subtropical circulation anomaly that enables moisture to be sourced from lower latitudes[9,24]. Atmospheric convection anomalies over the tropics and subtropics associated with the main modes of variability can trigger such coupled low–high latitude circulation patterns, such as the El Niño/Southern Oscillation (ENSO) or the Indian Ocean Dipole (IOD) on interannual timescales[20,25]. Such large-scale conditions that favour the formation of Antarctic ARs[7,12,19,25,26] could be used as a potential source for improved predictability of Antarctic ARs[25]. In particular, the phase of IOD–ENSO has a significant negative correlation with ARs in Ellsworth Land and a positive correlation in eastern Dronning Maud Land and the Ross Sea region significantly[25].

Modes of variability originating from the subtropics with a higher frequency than 1 year have also been shown to influence AR variability and strength; for example, the Madden Julian Oscillation[27], and/or weather and climate features such as convergence zones (for example, the South Pacific Convergence Zone)[24], and tropical cyclones that propagate to the mid-latitudes[23]. These linkages to the subtropics occur in part because deep convection can produce an effective Rossby wave source[28,29], triggering a poleward and eastward propagating wave that can either produce or enhance a pre-existing extratropical high–low couplet. These tropically forced circulation patterns can thus produce or enhance poleward moisture advection and also act as a bridge connecting the extratropical circulation to low-latitude circulation and moisture which leads to the ideal conditions for the most intense Antarctic ARs[30].

Synoptic-scale dynamics

Moving from the global-scale dynamics down to the synoptic-scale dynamics, the surface cyclone (to the west) and anticyclone (to the east) couplet accompanying Antarctic ARs develops in regions of divergence and convergence aloft associated with a mid-tropospheric trough–ridge couplet[8,9,19,26,31] (Fig. 1a). In addition

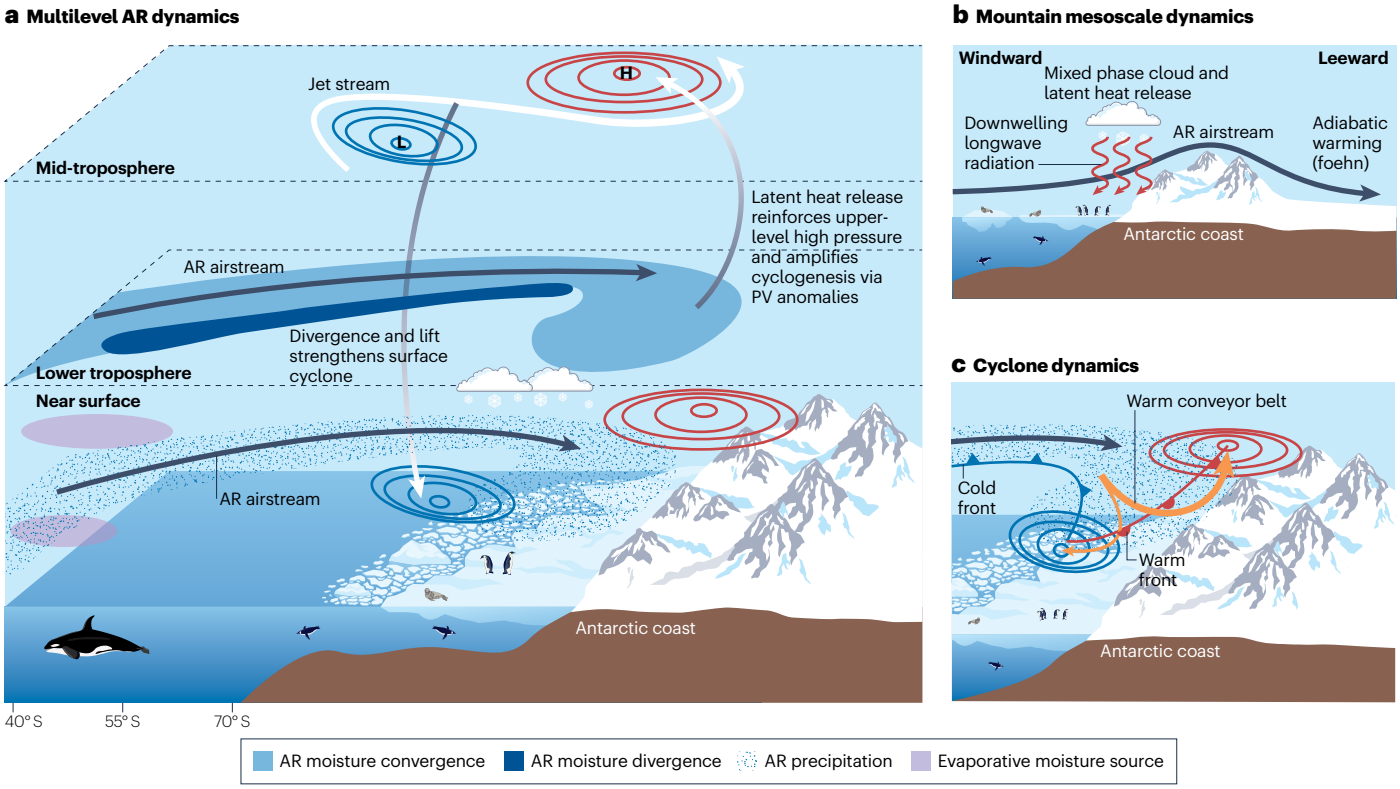

Fig. 1 | The dynamics of a landfalling Antarctic AR. a, Multilevel atmospheric river (AR) dynamics, from the surface, through to the lower troposphere and mid-troposphere. Mid-latitude sources of moisture are transported towards the polar latitudes by an AR (grey arrow), resulting in latent heat release of AR moisture. When the latent heat release occurs, it amplifies the polar jet stream (white arrow) and cyclogenesis via potential vorticity (PV) anomalies. **b**, Mountainous meso-scale dynamics typically observed in coastal regions such as the Antarctic Peninsula, focusing on thermodynamic processes. Mixed-phase clouds along the windward coastline heat the surface through downwelling longwave radiation (red arrows). When the AR airstream crosses mountainous terrain, it descends and warms adiabatically creating a foehn wind on the leeward side. **c**, Cyclone (synoptic-scale) dynamics demonstrating the pathway of the AR airstream as it lifted isentropically in the warm conveyer belt (orange arrows) over the warm front and eventually reaches the anticyclone (high-pressure area), causing the cyclone to intensify. ARs, through the poleward transport of moisture and heat, substantially alter the dynamics and thermodynamics of Antarctic weather patterns when reaching the cold, and sometimes mountainous terrain, along the Antarctic coastline.

to the mid-tropospheric trough–ridge couplet, tropopause polar vortices can become embedded within broader troughs and serve as a potent synoptic-scale forcing mechanism for surface cyclogenesis[30,32]. Wave patterns associated with ARs (Fig. 1a) feature substantially larger amplitude (~40 dm for the corresponding ridge and trough) than their non-AR counterparts[8,9,19] and transport heat and moisture poleward towards Antarctica. As shown by upper-tropospheric potential vorticity advection in the vicinity of ARs[30], latent heat release from condensation and deposition within the AR further enhances the intensity of the downstream ridge within the middle and upper troposphere (Fig. 1a), prolonging the duration of an individual AR event or sometimes establishing a blocking pattern conducive to an AR family event, in which multiple ARs impact the same location over a short period of time[31]. A blocking high east of an AR is particularly conducive to high precipitation events in which an AR persists at a single location over time[12,31]. Thus, ARs tend to amplify the synoptic configurations that favoured their development, indicating a two-way coupling between the ARs and their environment[9,19,30,33].

Although strong ARs are associated with tropical moisture (see the previous section on large-scale dynamics), landfalling Antarctic ARs generally source their moisture via anomalous evaporation around 40° S (refs. 9,26,30), but this varies by longitude. Back trajectories of Antarctic ARs show moisture sourcing at 30° S for the AP[20], 40° S for Dronning Maud Land[26] and 30°–45° S (around the Great Australian Bight) for events in Adélie Land[30]. The AR moisture supply from anomalous evaporation at mid-latitudes is cut-off as the AR travels poleward and the cool ocean temperatures invert the air-sea temperature differential[9,26] (Fig. 1a).

Mesoscale dynamics

Once the corridor of enhanced meridional heat and water vapour transport reaches the Antarctic coast, it is lifted via isentropic ascent (no energy exchange with the environment) induced by the steep topography[7,26] (Fig. 1c) and the presence of katabatically generated cold air masses, that is, the flow of cold, dense air from the Antarctic interior to the coast, which resides near the Antarctic coast[34,35]. Along with the topography, the AR air mass can experience lift via the warm conveyor belt associated with the attendant surface cyclone[8,33] (Fig. 1c). Additional latent heat release from AR intrusions generates cyclonic potential vorticity anomalies in the lower troposphere, which further

enhance poleward moisture transport, promote ascent within the warm conveyor belt and favour the inland penetration of ARs. When ARs interact with regions of elevated topography, especially the coastal mountains of the AP, they often produce intense windward precipitation and cloud formation[36]. On the leeward side, ARs can induce substantial foehn warming (2–3 °C on average)[37,38] near the base of the mountain, which is enhanced via both intensified latent heat release and strengthened flow accompanying the AR-associated low-level jet[16,20,26] (Fig. 1b). Over the AP, strong ARs can channel moisture to the leeside through gap flow or spillover[39–41], influencing downward longwave and shortwave radiation based on cloud conditions. Further research is needed to fully understand the impacts of ARs on leeside mountain waves and the associated sensible heat flux[16,42], as ARs typically bring low-level jets and warmer temperatures.

Interaction of ARs with topography triggers various extreme weather phenomena, such as windward intense precipitation (~150 mm water equivalent per year)[7] and leeward high temperatures (10 °C in extreme cases)[40] owing to the AR-induced foehn. Thus variability in AR extreme weather patterns is influenced by the connectivity between local topography and regional circulations[20,39,40,43]. For instance, the AP region has experienced increasing AR-induced foehn warming, attributed to the positive trend of the Southern Annular Mode. Substantial AR and foehn-induced melt events usually arise from strong vertical wind shear in (north-)easterly airflows. Furthermore, foehn warming induced by AR intrusions has been observed in the eastern Ross Ice Shelf, Amundsen Sea Embayment and Vestfold Hills in East Antarctica, typically associated with regional circulation patterns such as the Amundsen Sea Low[35,43–45].

Microphysical processes

Antarctic ARs are associated with complex cloud and precipitation microphysics. These microphysical processes are related to the larger-scale atmospheric dynamics discussed in the previous sections and relate to the high moisture content, increased temperatures and specific aerosol properties of Antarctic ARs. One of the key features of Antarctic ARs is the presence of mixed-phase clouds with a large amount of supercooled liquid water causing a strong increase in the downwelling longwave radiative fluxes that warm the surface[10,20,40]. Complex interactions between the ARs and AP topography have been shown to cause cloud clearance (with increased downwelling shortwave radiation) in some regions and gap flows with cloudy conditions (increasing downwelling longwave flux) in other regions[40]. On the opposite side of the ice sheet, at Davis station in East Antarctica, orographic gravity waves generated during an AR event intensified snowfall formation owing to updrafts and turbulence in the middle troposphere, but at the same time caused sublimation below about 1,000 m a.s.l. because of the relatively dry foehn effect[35]. Thus, the AR event impacted precipitation microphysics in the vertical profile, modifying spatial distribution of snowfall amount at the surface[35]. Substantial increases in the cloud liquid water path during warm–moist intrusion events, typically associated with ARs, have been recorded deep into the East Antarctic interior (from 0 to 50 g m^{-2} in one case at Dome C)[46]. In particular, during the record-breaking AR event affecting East Antarctica in March 2022, a strong increase in cloud liquid water path and associated cloud longwave warming of the surface were responsible for the largest positive anomalies in the surface energy balance[23].

The importance of aerosols for cloud microphysics was noted following the 2018 AR over the Southern Ocean and Tasmania[47], particularly how these microphysical processes enable the ARs to reach Antarctica. The aerosol interaction occurs via ice nucleation in the upper part of the AR (sourced from tropical moisture), which enhances hydrometeor production in the lower part of the AR (primarily sourced from mid-latitude moisture). The ice nucleation influences and enhances hydrometeor production in the lower part of the AR, which primarily comprises moisture sourced from the mid-latitudes[47]. Bioaerosols have an especially important role in ARs over the Southern Ocean: sourced from the mid-latitude ocean, they act as ice-nucleating particles over high latitudes even in relatively high temperatures (above −10 °C). Strong ARs reaching the AP are associated with aerosol transport events, particularly of black carbon and dust, which play crucial roles in liquid and mixed-phase clouds, with black carbon serving as cloud condensation nuclei and dust as ice-nucleating particles[48]. In summary, aerosols within ARs can influence ice–liquid partitioning, alter cloud albedo and optical depth (thus influencing cloud radiative forcing and precipitation timing), elevate aerosol optical depth by water uptake in hygroscopic aerosols (directly influencing surface radiation) and precipitate out (yielding darkened snow and ice surfaces).

Beginning in the subtropics with perturbations in convection and cyclonic activity to terminating over the Antarctic coastline delivering copious amounts of heat, moisture and aerosols, there are many factors that determine the life cycle of Antarctic ARs. Understanding the variability in these factors is crucial for understanding the climatology of AR activity around Antarctica.

Climatology and variability

Antarctic ARs are generally rare events, typically occurring around 3 days per year across Antarctic coastal regions, but with high degrees of interannual variability and regional trends. Measurements of AR variability are sensitive to the choice in the detection method (Box 1). However, it is understood that AR variability often controls precipitation patterns across the AIS. This section discusses Antarctic AR frequency, interannual variability and both historical and future trends.

AR frequency

Antarctic AR frequencies are based on polar-adapted AR detection algorithms that emphasize poleward oriented integrated water vapour and the meridional component of integrated vapour transport; both at the relatively high 98th percentile climate threshold[7]. ARs exhibit a generally zonally symmetric frequency over the Southern Ocean that decreases progressively when approaching the Antarctic coastline[7], likely due to their lower-latitude moisture origins. In quantitative terms, if to sum up all hours of AR passing at specific location, ARs typically occur around 3 days per year across Antarctic coastal regions with notable variability. For instance, the Ross Sea has the lowest frequency of around 1 day per year, whereas the AP and Dronning Maud Land have the highest, up to 3 days per year (Fig. 2a). Seasonally, AR activity generally peaks during the austral winter (June, July, August), with regions such as the AP and Dronning Maud Land experiencing around 1 day per year of AR activity. During the austral summer (December, January, February), AR activity is lower, contributing less than 0.5 days per year in many regions across Antarctica (Fig. 2a). Moisture intrusions become more prominent during winter when based on a relative threshold, despite the ARs transporting less moisture and suggesting a drier atmospheric condition during this season[7]. Compared with global AR detection tools (ARDTs), polar-specific ARDTs have a higher frequency of AR occurrences over the Antarctic interior (0.5% greater)[25].

Box 1 | Antarctic AR detection and ranking

This box presents the detection and ranking techniques that have been developed to characterize atmospheric rivers (ARs) specifically in Antarctica. A diverse suite of AR detection tools (ARDTs) is currently being used by the AR community, each designed with a specific purpose or science question. Many of these tools are described by the Atmospheric River Tracking Method Intercomparison project (ARTMIP)[116,117]. Using values such as integrated vapour transport (IVT) or integrated water vapour estimated from gridded data sets such as reanalyses or models, ARDTs typically apply a moisture threshold (fixed or relative) to determine whether an AR condition existed. Owing to the lower water vapour saturation capacity of the colder troposphere in Antarctica, detecting ARs there requires lower moisture thresholds. Moreover, for an AR to make landfall in Antarctica, particularly in areas other than the western Antarctic Peninsula (AP), a dominant meridional moisture transport is required. Two Antarctic-specific ARDTs have been developed for East Antarctica (in 2014 and 2020)[12,118] and for the entire Antarctic (in 2019, updated in 2021)[7,10]. The former[12,118] algorithm is based on the Clausius–Clapeyron relationship and threshold applied uses saturation specific humidity compared with the mean integrated water vapour over corresponding latitude at a given moment in time. The latter[7,10] has two threshold options, based on integrated water vapour or on a meridional component of IVT identifying meridionally dominant ARs, defined as greater than 98th percentile compared with monthly climatological means. Both polar algorithms have geometrical criteria with length >20° equatorward (>2,000 km length), with an allowance of a more zonal orientation for better detection over the AP in the updated version of ref. 118. Compared with global ARDTs, Antarctic-specific methodologies better identify and constrain ARs impacting the ice sheets and shelves of the continent, whereas global ARDTs appear to be too permissive when applied to Antarctica[25]. Historical AR detection over Antarctica has been typically based on ERA5 (ref. 119) and MERRA-2 (ref. 115) reanalyses (showing the best representation of temperature and humidity fields in Antarctica) with more significant differences compared with global algorithms than between the two reanalyses[7,10,25]. AR detection frequency is typically lower in lower resolution reanalyses (~2.5° spatial resolution) but tends to converge in data sets with resolutions between 0.5° and 1.0° (ref. 10). Thus, the polar-adapted ARDTs are necessary tools for creating a climatology of Antarctic AR frequency.

In addition to the ARDTs that identify ARs as objects in space, the AR scale developed in ref. 120 ranks ARs based on both their intensity and duration for specific locations at middle latitudes. An extended version of the AR scale tuned for the polar regions was introduced in ref. 50: for a specific location in a polar region, an AR event is ranked based on the duration of the AR condition (IVT ≥ 100 kg m^{-1} s^{-1}) and the intensity (maximum IVT). The forecasts of the polar AR scale were used in guiding radiosonde launches during the Year of Polar Prediction in the Southern Hemisphere (YOPP-SH)-targeted observing periods[114].

By contrast, other global ARDTs identify a greater number of ARs over the Southern Ocean (~5% greater)[25].

Interannual variability

ARs present a strong interannual variability on a regional scale. According to the detection algorithm in ref. 7, this interannual variability is significantly positively correlated with annual precipitation across most regions of the AIS, implying that AR variability controls precipitation variability[49]. However, if all AR landfalls are integrated across the entire Antarctic coastline, the interannual variability only exists for the most intense ARs (according to the polar AR scale)[50] and disappears when counting all ARs.

The regional interannual variability in AR frequency is influenced by regional modes of variability, such as the Southern Annular Mode[7,51–54], and broader teleconnections. As mentioned earlier, the main modes of variability link Antarctic AR variability with tropical convection behaviour. Teleconnections exist on both decadal timescales, such as the Pacific Decadal Oscillation[54,55], and interannual timescales, such as Pacific South American Modes[51,56] and IOD[52,53]. These modes modulate the coupling between extratropical high–low pressure systems and subtropical circulation patterns, enhancing poleward moisture transport from lower latitudes into Antarctica, which in turn affects AR frequency and intensity. Overall, most modes of natural variability influence AR activity in West Antarctica more than in East Antarctica. Additionally, when interannual modes such as the IOD and ENSO are in phase and positive, the associated warming surface air temperatures contribute to enhanced moisture fluxes into the atmosphere and therefore cause increased moisture availability and precipitation in ARs that ultimately impact Antarctica[25].

Historical changes

According to the polar AR scale, when averaged along the entire Antarctic coastline from 1979 to 2022, there is a slight but not statistically significant increasing trend in the average frequency of landfalling ARs[50]. However, regional trends are apparent, like on the AP where there is a statistically significant increasing trend (+0.89 ARs per decade, 90% confidence interval). This increasing trend is accompanied by substantial interannual variability increase, especially since the early 2010s, consistent with findings indicating an increasing trend in AR frequency over West Antarctica[7,31]. The increasing trend of AR frequency over the AP and parts of West Antarctica might be related to the poleward shift of extratropical cyclones, which are critical to AR activities[57–59].

AR frequency trends from 1980 to 2020 show substantial regional variation over individual glacier basins (Fig. 2b), based on the detection algorithm of ref. 7. The basins with positive precipitation trends are significantly correlated with regions of positive AR frequency trends such as Ellsworth Land in West Antarctica, which saw an increase of +20% to +30%, and Dronning Maud Land in East Antarctica, where AR frequency rose by about +20% to +30% during the 1980–2020 period. Conversely, Wilkes Land exhibited a negative yet insignificant AR trend of around −5% to −10%, which corresponds with a decrease in snowfall during the same period[7,31,49]. This negative trend is occurring against the backdrop of an observed poleward shift of the Southern Ocean storm track which brought ARs closer to the Antarctic continent[60].

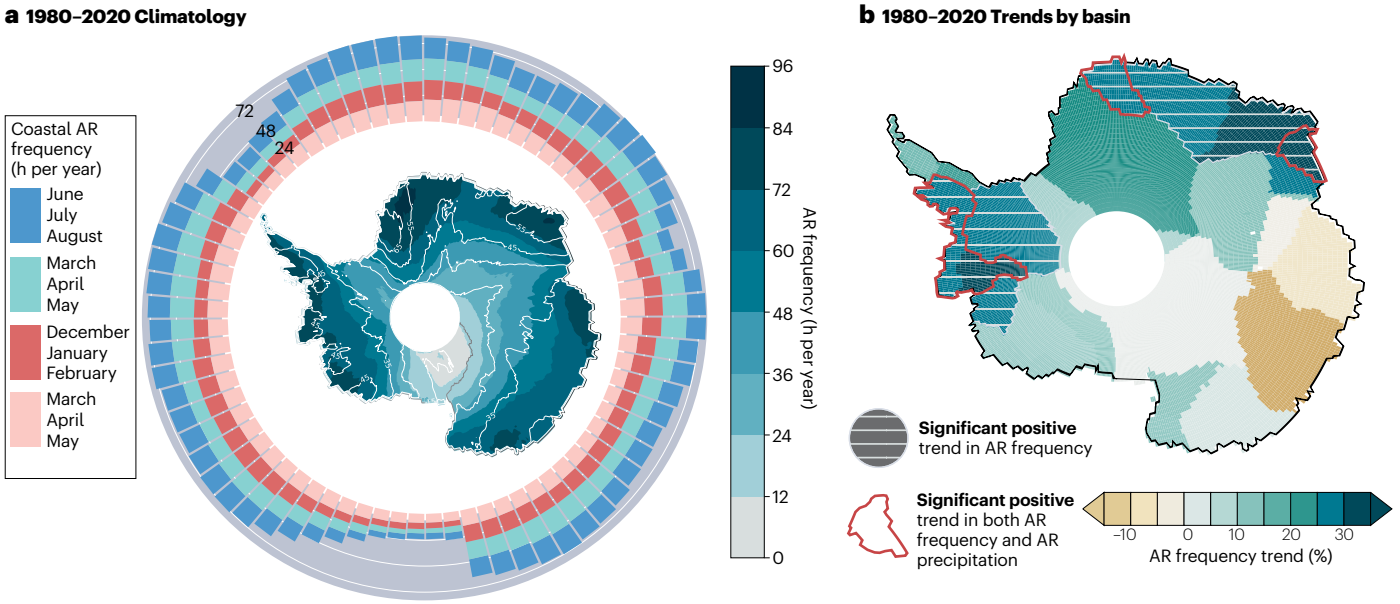

Fig. 2 | AR frequency, trends and projections. a, Atmospheric river (AR) frequency (h per year, 1980–2020; teal shading) derived from the algorithm and MERRA-2 (Modern-Era Retrospective Analysis for Research and Applications, version 2)[115] reanalysis of ref. 7. Interannual variability is shown in white contours (h per year). Coastal (based on ice sheet and shelves) AR frequency is shown by longitude and grouped by season. **b**, Relative change in AR frequency (%) by individual glacier basin from 1980 to 2020 is shown with shading, also based on the MERRA-2 reanalysis of ref. 7. Hatching indicates a linear fit of AR frequency (horizontal) or AR precipitation (vertical) per basin from 1980 to 2020 that has a P value <0.05. AR precipitation trend values are not shown. Despite being rare events, positive trends in AR frequency are responsible for increased snowfall in West Antarctica and Queen Maud Land during the 1980–2020 period.

Projected trends

Generally, global AR frequency and intensity are expected to increase considering that moisture availability will increase simply owing to the Clausius–Clapeyron relationship[61], although these changes should not occur uniformly in polar regions[62]. Future projections of global AR frequency and impacts are sensitive to the choice of ARDT. The choice of detecting ARs using a fixed-relative methodology (historical thresholds for all simulations) or a purely relative methodology (time-varying thresholds) will determine the strength, and even sign, of the future AR characterization and impacts[61,63]. Fixed thresholds based on historical conditions could lead to a substantial overestimation of future AR events relative to the background moisture field[64]. With that in mind, AR frequency in the Southern Ocean around Antarctica is projected to increase by 5–20% by the end of the twenty-first century following the SSP585 scenario according to a CMIP6 multimodel mean. A substantial increase in ARs is expected in Antarctica even in regions where the count is zero in the present climate[63].

Although ARs are a rare phenomenon over the Antarctic continent, they are critically important for controlling precipitation patterns across most of the AIS. Their frequency and intensity should increase in the future. Year-to-year variations in AR activity over a certain region of Antarctica can have drastic impacts regarding snowfall, surface melting and other mass balance processes.

Impacts and extremes

ARs present circulation anomalies over the Southern Ocean that can cause substantial impacts on surface variables over the Antarctic continent, for example, through precipitation, winds, temperature and ice melting. The dominant impact of ARs is to contribute precipitation to the AIS (primarily in the form of snowfall), positively impacting the ice sheet mass balance. By contrast, AR-attributed rainfall, melt and winds can have destabilizing impacts on Antarctica's ice shelves and sea ice. Although measurements of AR impacts are scarce across Antarctica, a combination of remote sensing, observational campaigns and snow measurements help to verify many AR details simulated in models (Box 2). This section aims to provide a comprehensive review of the impacts of ARs on AIS mass balance and local ecosystems, which are important for projecting climate change impacts in these regions.

Surface mass balance and melt

The AIS mass balance (−92 ± 18 Gt per year over 1992–2020 with an increase of loss to −150 ± 43 Gt per year over 2012–2016)[65] is commonly defined as the balance between the surface mass balance (SMB; ~2,329 ± 94 Gt per year over 1987–2015)[66] and the discharge of ice from the grounded AIS into the ocean[67,68]. The SMB represents the balance between surface mass gained through precipitation (snowfall and rainfall), condensation and blowing snow deposition, minus mass lost through runoff, sublimation/evaporation and blowing snow erosion[67]. The dominant impact of ARs on the Antarctic SMB is precipitation, most often in the form of intense/extreme snowfall[7,69]. From 1980 to 2020, ARs contributed 13% (±3%) of the total Antarctic precipitation (including ice shelves) — an order of magnitude higher than their frequency (1–1.5%)[7,49]. AR relative contributions to the total snowfall are highest across Dronning Maud Land and Wilkes Land (~20%), lower in West Antarctica (~10%) and lowest at high elevations in the East Antarctic Plateau (0–5%)[7,49]. AR impacts may be underestimated over the East

Antarctic Plateau as ARs crossing the continent are rarely captured by detection algorithms[7,25].

The contribution of ARs to interannual variability in precipitation varies locally over the AIS (Fig. 2b). As an example, the March 2022 AR event produced 98 Gt of precipitation (2.9 standard deviations above the monthly mean), localized entirely in East Antarctica (Box 3). However, ARs impact precipitation almost everywhere over Antarctica. In some regions of West Antarctica, such as the Amundsen Sea Embayment and Marie Byrd Land, ARs are associated with 29% of the interannual variability in total precipitation, based on the correlation between detrended annual AR and total precipitation from 1980 to 2019 (ref. 31). In austral winter 2019, ARs in this area were associated with 26% of all satellite-observed surface height increases owing to snowfall[70]. In austral summer 2020, a series of three AR events (an AR family event) that made landfall in the Amundsen Sea Embayment over 10 days caused 9% of the total precipitation that year, whereas the annual mean contribution of ARs to the total precipitation in that region is 11% over 1980–2020[31]. In drier regions, more particularly over East Antarctica, ARs control a large part of precipitation variability, as, for instance, in Dronning Maud Land, where ARs explain 77% of the variance in total precipitation[8]. In Dronning Maud Land in 2009 and 2011, four and five impactful ARs contributed up to 80% of the SMB anomaly in those years, respectively[12] (Fig. 3).

This strong control of ARs on precipitation has logically meant that recent increases in AR frequency, occurring almost everywhere in Antarctica except in Wilkes Land (Fig. 2b), have impacted precipitation trends[49]. However, precipitation has responded with distinct spatiotemporal trends[7,36]. From 1980 to 2019, AR precipitation in the Bellingshausen sector in West Antarctica, parts of Dronning Maud Land and the west coast of the Ross Sea shows a linear trend exceeding 50% relative to the 1980–2019 mean[49].

At the same time, ARs can also have a negative impact on the Antarctic SMB by generating surface melt and runoff. ARs are associated with the majority of extreme melt events in West Antarctica and on the AP. Climatologically, ARs are responsible for 40% to nearly 100% of the total summer surface melt across the Ross Ice Shelf and higher elevations of Marie Byrd Land and 40–80% of the total winter surface melt on the AP[10]. These ARs often bring warm air advection and high moisture content, leading to enhanced cloud formation and precipitation, which release latent heat and trigger thermodynamic foehn warming[16,36,40,43] (Figs. 1b and 4). The high moisture in ARs can further amplify the melt events through increased downward longwave radiation from thick clouds with high liquid and ice content[10,36,40,71,72] (Fig. 4). In East Antarctica, an AR's control over melting is less straightforward, as other types of situations can produce summer melting in coastal regions, but it is a major control for melting events occurring far inland

Box 2 | Measurement techniques of Antarctic ARs and their impacts

Targeted observational campaigns are aimed to capture the extreme nature and high temporal and spatial resolution of observed Antarctic atmospheric rivers (ARs), as well as their impacts. Observing ARs and their impacts directly, especially in the harsh and remote polar regions, requires sophisticated remote sensing and in situ measurement strategies. Satellite remote sensing, particularly using microwave radiometers, is crucial for capturing the spatial dimensions and elevated moisture content, cloudiness and precipitation during AR events across large scales[20,47,121,122]. However, detection limitations specific to the polar regions (for example, large biases in microwave and visible measurements over ice surfaces), strong spatiotemporal variability during AR events and limited satellite overpasses hinder their application for AR detection and characterization over Antarctica[123].

Satellite remote sensing has also been applied to analyse impacts of ARs on the Antarctic surface mass balance and snow properties, including drastic sudden increases in ice sheet elevation owing to anomalous snowfall in West Antarctica using ICESat-2 laser altimetry[70], extensive surface melt extent over the Antarctic Peninsula (AP)[20] and snow grain size increase in East Antarctica using microwave radiometer observations[124]. Snow accumulation reconstruction using Global Navigation Satellite System interferometric reflectometry also showed the importance of extreme snowfall events affecting the Amundsen Sea Embayment during ARs[70].

Targeted[20,35,118] and opportunistic[71,124] ground-based observations provide important high-resolution measurements of near-surface meteorology, clouds and thermodynamic state of the troposphere during AR events. High-resolution ground-based remote sensing of precipitation using radars proved useful in capturing anomalous snowfall events and their vertical structure[12,35] as well as the growing importance of rainfall during ARs[20,125]. Planned campaigns organized as part of large observational programmes, such as the YOPP-SH, have used radiosondes to show the extreme impact of ARs on the temperature, humidity and wind profiles and to improve AR forecasting skills in weather and climate models, together with automatic weather stations including longwave and shortwave radiation measurements used to constrain the surface energy budget when ARs make landfall[40,114,118,125]. The winter YOPP-SH observing period in 2022 successfully showed the importance of multinational efforts in enhancing ground-based observations and merging with modelling efforts to conduct targeted observations of the Antarctic AR and their impacts on the surface mass and energy budget.

Ongoing observational efforts are also applied to understand impacts of ARs inside the Antarctic snowpack and ice cores. Past constraints on AR impacts recorded in snow stratigraphy are challenging to interpret because of the connected nature of precipitation and the recorded proxy (for example, layer thickness and layer chemistry). UHF/K-band ice-penetrating radar observations have been used to constrain distributed patterns of melt in Greenland[126,127] and should be used to map melt events across Antarctica using contrasts in dielectric permittivity recorded in firn. Targeted shallow coring efforts near the periphery of the ice sheet are also underway and could facilitate analysis of AR impacts on oxygen isotope fraction[128]. Isotopic records (vapour and precipitation) on daily resolution could be sufficient to simply detect an AR, given the characteristic synoptic period of AR events[23]. But for process studies, to understand and decompose the different phases that make up those extreme events in both measurements and models, hourly resolution is required as a minimum[98,129].

Box 3 | The March 2022 East Antarctica extreme AR

From 15–19 March 2022, an extremely intense atmospheric river (AR) made landfall in East Antarctica that triggered a subsequent heatwave with temperatures 30–40 °C above normal across an area roughly half the size of Europe (see the figure).

The origins of this AR were traced back to tropical convection and the occurrence of three successive cyclones across the Indian Ocean and of tropical-temperate troughs over the African landmass[130–133], which advected record-high plumes of tropical moisture into the mid-latitudes. This tropical convection helped to initiate a Rossby wave propagation leading to the formation of an intense blocking anticyclone centred south of Tasmania. The block extended poleward which directed the subtropical moisture towards Antarctica in the form of an AR family event[31]. The AR, coupled with a warm conveyor belt near the coastline, helped to lift the moisture to the tropopause, causing substantial potential vorticity anomalies in the high troposphere, which reinforced the atmospheric blocking deep into East Antarctica[30,134]. These combined factors pushed a record-shattering moisture flux poleward (an Aqua Moderate Resolution Imaging Spectroradiometer, true colour image from 17 March 2022) (see the figure), where IVT from this AR was 8.7 standard deviations from the mean AR IVT across East Antarctica and the event ranked as an AR category 4 on the polar AR scale[50]. The accompanying upper-level warm air advection into the continent and longwave radiation from liquid-laden clouds eroded the typical surface temperature inversions over the ice sheet.

This AR and subsequent heatwave led to an area of 3.3 million km^2 in East Antarctic to exceed March monthly temperature records. Meanwhile, a new all-time high temperature record of −9.4 °C was set near Concordia Station on 18 March 2022, despite March typically being a winter transition month. This event accounted for 32% of total Antarctic ice sheet (AIS) precipitation during March, which saw highly anomalous rain (+0.49 Gt) and surface melt (0.5 Gt) along coastal areas, although snowfall vastly counterbalanced the losses due to melt (+42.5 Gt). At Dome C station, isotope measurements revealed a distinct summer-like signature, whereas cosmic ray measurements were attenuated by the anomalous atmospheric moisture; both showing the implications for paleoclimate studies[135]. Finally, an extratropical cyclone west of the AR landfall likely triggered the final collapse of the already critically unstable Conger Ice Shelf, while further diminishing land-fast ice, which was already at a record minimum[14,23].

Overall, the AR event largely contributed to 2022 being a rare positive mass balance year for the entire AIS, thus slightly mitigating the AIS's contribution to sea-level rise[18]. However, the temperature extremes also raised concerns of potentially dire consequences for ice sheet stability if a similar magnitude event happens over a sensitive ice shelf in West Antarctica during the summer melt season.

AR event, 17 March 2022

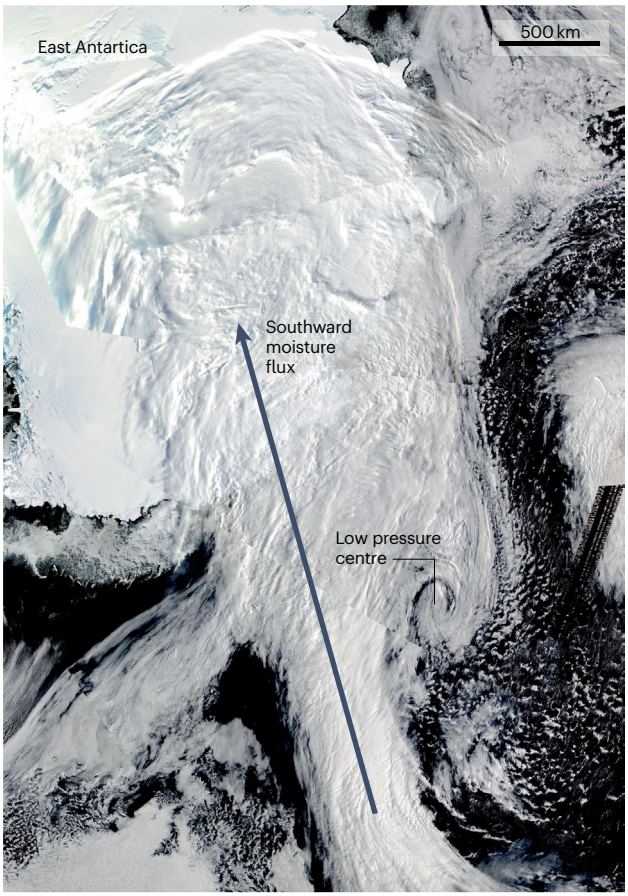

and outside the summer period. For instance, the March 2022 AR event produced record temperature anomalies of 30–40 °C across the AIS[23], resulting in brief surface melt over an area of ~40,000 km^2 on the grounded ice sheet as well as intense surface melt at the margins (+40% greater than average March melt) (Box 3). Even where surface melt does not lead to runoff (contributing negatively to SMB), it can directly impact the structure of the firn (the porous multiyear snow which has not yet compacted into glacial ice under its own weight)[73]. Firn has a depth which ranges from metres to nearly 100 m on the AIS, exists on both the grounded ice sheet and floating ice shelves and includes complex hydrology and ice features. When surface melt occurs on ice shelves, liquid water will percolate and potentially refreeze until it fills the empty pore space in firn[74]. Surface melt water also amplifies shortwave radiation absorption, releases latent heat during refreezing, accelerates snow ageing and facilitates melt pond formation through impermeable ice lenses[73–75].

One simple measure frequently used to estimate how the balance between melt and accumulation impacts firn is 'melt over accumulation', which approximates the nonlinear impacts of melt[75,76]. By this measure, the ice shelves around Antarctica will become increasingly vulnerable in the future[77]. Ice shelves are vulnerable to surface melt as liquid water can produce aquifers and surface/subsurface streams that fill crevasses with water, driving these crevasses to penetrate deeper into the ice and in some cases all the way through the ice shelf[73,74] (Fig. 3). This process, known as hydrofracturing, contributes to destabilizing ice shelves[73,78]. A striking example of the links between ARs and

hydrofracture occurred in January 2008, which resulted in substantial runoff and the disintegration of land-fast ice in the Larsen A and B embayments, culminating in a major calving event[36].

In addition to ice shelf hydrofracture, ARs are also associated with ice shelf calving and collapse through sea surface-slope-induced and wave-induced fracture, when surface winds associated with AR cyclones trigger ocean surge and swell at the coast[14,36,79,80]. The transition between onshore and offshore winds causes ocean surge to shift from the ice shelf front to offshore, leading to abrupt changes in sea surface slope, which causes the ice shelf to flex. AR-induced ocean swell was a key driver of the collapse of the Conger ice shelf during the March 2022 East Antarctic AR event[14,81] (Box 3). Offshore winds associated with AR storms also have an important role in the rapid distribution of fast sea ice abutting ice shelves away from calving fronts, which can reduce the buttressing effect and increase glacier discharge and the likelihood of calving events, such as the collapses of Larsen A and B ice shelves in 1995 and 2002, as well as the Larsen B fast ice breakout in January 2022 (refs. 36,82) (Fig. 3).

As a summary, although present-day large-scale snowfall impacts mass gain most directly, ARs also produce losses through melt with nonlinear impacts on ice shelf destabilization, whose contribution to the total mass balance, currently small, could become significant and even unpredictable and uncertain. Moreover, ARs also initiate synoptic and mesoscale conditions enhancing this nonlinearity. As an example, foehn winds, frequently driven and intensified by ARs, can produce intense melt events over the vulnerable Larsen C ice shelf, sometimes leading to melt over nearly the entire surface[36], like in January 2020 with 7.2 Gt of meltwater[36], in February 2020 (ref. 83), and an unprecedented winter melt event in 2016 (refs. 38,84) (Figs. 3 and 4). Furthermore, intense surface melting on the Larsen Ice Shelf associated with ARs can be further intensified through the formation of optically thin liquid-containing clouds, permitting the transmission of shortwave radiation during the day, while enhancing longwave warming during the night[10,20,36,42] (Fig. 4). In addition to nonlinear impacts on local synoptic conditions, ARs can have impacts on other parts of the earth system, including sea ice and ecosystems.

Sea ice

ARs are associated with a decline in sea ice concentration (SIC), sea ice advection and polynya openings[15,85] and have been shown to amplify large-scale warm air advection[11,15,86,87] and cause changes to downwelling longwave radiation over sea ice[11,15]. The impacts of ARs on the surface energy balance over sea ice are similar to those on land ice, although ARs can also generate a significant amount of warm snow over sea ice in austral winter which increases the insulation capacity of ice and contributes to its melt[15]. In the marginal ice zones, ARs contribute to a nearly 10% reduction of sea ice concentration per day across all seasons[11,36] and can remove nearly 50% of sea ice concentration during a single event[88].

A more holistic understanding of AR impacts on sea ice can be gathered from jointly considering ARs and their associated cyclones. ARs supply additional water vapour, enhancing latent heat release and cyclone intensity[15,88]. The combined system leads to wind-driven and swell-driven poleward sea ice advection[36,88] (Fig. 4) and increases wind stress on the ice cover[15]. Cyclones featuring ARs may lead to a dipole of sea ice variability, but the long-term frequency of this effect remains understudied[14,88].

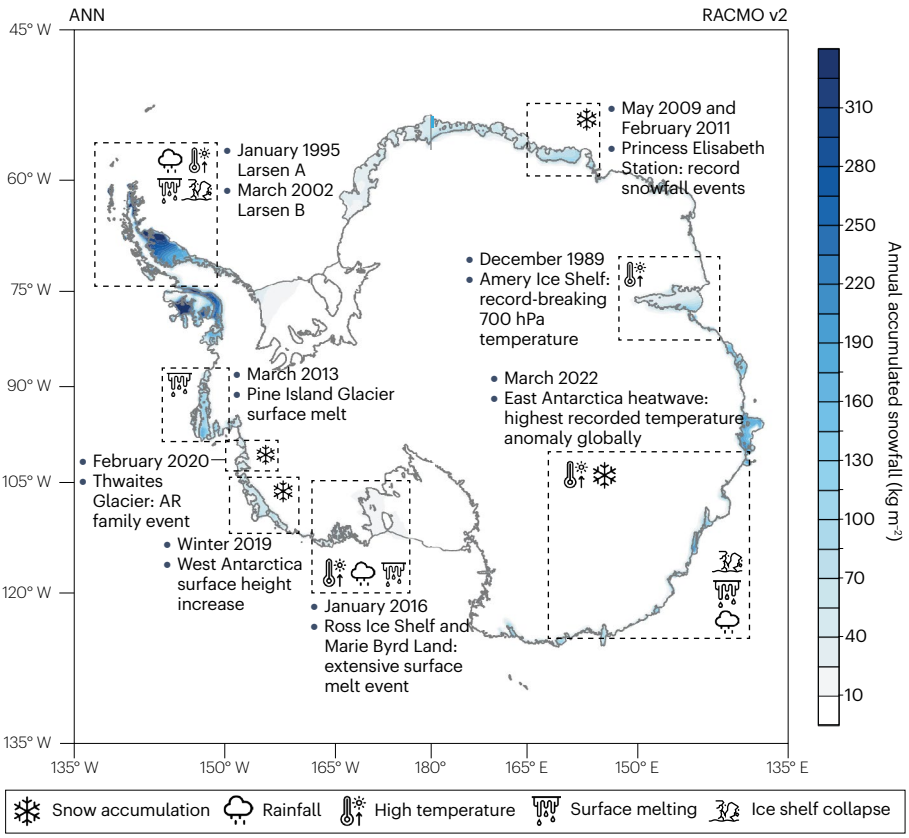

Fig. 3 | Antarctic AR extremes. Impacts of atmospheric river (AR) events that have made landfall in Antarctica between 1980 and 2022. These were notable AR-related extreme events discussed in the literature covering impacts such as intense snowfall, rainfall, high temperature extremes, surface melting and final ice shelf collapse. Annual accumulated surface melting data are based on the monthly average Regional Atmospheric Climate Model version 2 (RACMO v2) data set[76], featuring documented AR-triggered extreme weather events from previous studies. Although these recorded extremes represent high-impact events with long-lasting consequences, these are not meant to be an exhaustive list as many Antarctic AR-related extreme events have gone unstudied.

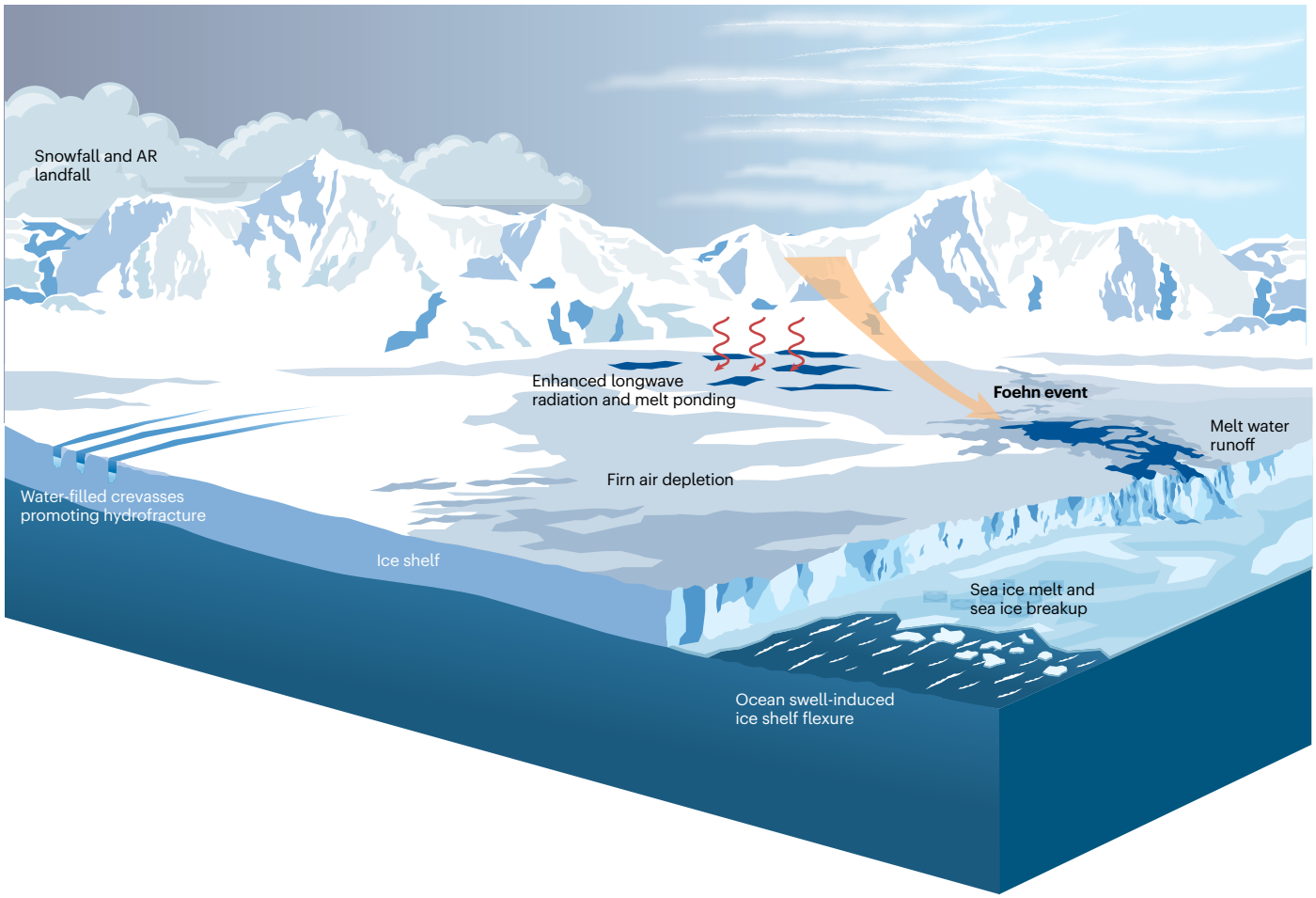

Fig. 4 | AR impacts. Typical observed impacts from atmospheric river (AR) landfalls in regions of mountainous terrain such as the Antarctic Peninsula. These include windward snowfall accumulation to leeward foehn wind and downwelling longwave radiation resulting in intense surface melt. On an ice shelf, these can lead to melt pond formation and eventual hydrofracturing while disintegrating the sea ice buffer along the ice shelf front. Thus, AR events can cause impacts on ice surface mass balance from the margins to the interior.

In pack ice and coastal regions, the dynamic and thermodynamic effects of ARs generally counterbalance each other, leading to minimal SIC changes in the inner ice zone[11]. AR-driven poleward sea ice transport reduces SIC in pack ice regions[11] (Fig. 4). However, thermodynamic processes refreeze ice as it drifts, offsetting the dynamic effects[89]. Near the coast, compact ice is advected from the pack ice zones and can experience some ridging[90], contributing to minor reductions in coastal SIC during AR events[11]. Furthermore, the decrease in sea ice and the associated swell dampening influence following the passage of ARs have been linked to the final collapses of the Larsen A and Larsen B ice shelves in the AP and the Conger ice shelf in East Antarctica[14,36,79,81,91,92].

Ecosystem impacts

Surface melt impacts of ARs can also extend beyond large ice shelves, affecting maritime Antarctic islands through extreme warm and foehn events[93,94]. Heavy precipitation resulting from ARs can also lead to dramatic impacts on living species around Antarctica, as observed at the Dumont d'Urville station in 2014, when a strong AR led to the complete breeding failure of the Adélie penguin colony[95]. The March 2022 AR caused extreme weather in the Antarctic Dry Valleys, with observed temperatures 25 °C above average conditions[23]. These extreme conditions manifested as a foehn wind event off the Polar Plateau, similar to AR influences in other regions of Antarctica[93,94]. Record austral autumn temperatures drove mobilization of liquid water in soils and sediments and likely the reactivation of resident biota (cyanobacteria mats and soil invertebrates) at a time when organisms are entering winter dormancy[96]. Biotic responses to unseasonable warm and wet conditions may have influenced diversity and life-history characteristics of biotic communities.

Water stable isotopes

Understanding the broader impact of ARs, particularly their role in influencing precipitation, requires additional analysis such as examining water stable isotopes. In polar regions, water stable isotopes are traditionally used as proxies for temperature reconstructions. Studies of the impact of extreme precipitation events are often limited to precipitation-weighted temperature[97]. Even in the specific case of ARs,

studies focusing on water vapour show that as a first-order parameter (d18O or dD of vapour), the isotopic signal is strongly correlated with temperature[14,98,99]. At second order (deuterium excess of vapour), a potential signature was observed for the first time in a recent winter-time AR event in the AP[99] similar to the event reported in Greenland[100]. However, determining the natural variability of ARs is a key element in future perspective analysis. As they are associated with heavy precipitation and significant isotopic anomalies, we expect ARs to imprint on ice core records[14,100]. This is important not only for reconstructing past climate conditions but also for understanding the impacts of current AR events. The March 2022 AR event, for example, offers a contemporary case study in which these methods can be applied to analyse both immediate and long-term impacts on the Antarctic environment. Another possible avenue for finding an AR signal in paleoclimate records is through the attenuation of cosmic ray transport in normally dry environments. As observed for the first time during March 2022, a saturated environment caused by an AR interrupted measurements of neutron fluxes during a magnetic solar event[14] (Box 3). This is relevant for past climate reconstructions as cosmic rays impart a beryllium-10 (B10) signature on the snow surface, which is used in ice-core dating, thus implying that past AR activity could possibly be inferred by the imprint they leave on the beryllium-10 (B10) signature and may be used to determine the occurrence and timing of past AR events in Antarctica. One last potential method of detecting an AR signal in paleoclimate records is by tracing polar aerosol ARs[48], although no robust proxy is currently available to define anomalous horizons as resulting from an AR event.

Projected impacts

Future AR impacts on the Antarctic environment will be the product of changes to the physical characteristics of ARs and their large-scale atmospheric drivers, combined with their interactions with the changing state of the Antarctic cryosphere. Here, we describe projected AR impacts to the grounded AIS SMB, ice shelves and sea ice.

Over the grounded AIS, projected SMB evolution critically depends on the emissions pathway that society follows. In low-emission to high-emission scenarios, increases in net precipitation over the AIS owing to temperature increases, and associated atmospheric moistening and atmospheric dynamics changes, are projected to offset the SLR by 19–79 mm (ref. 101) and compensate for warming-induced increasing melt[102,103]. The projected future snow accumulation increase is expected to be strongly controlled by short-term synoptic-scale events (for example, storm systems) such as ARs[104]. More frequent and intense rainfall resulting from blocking and moisture intrusions is projected to impact coastal Antarctica and new regions by the end of the century with a 7.6 mm per year average increase in rainfall over the AIS[105]. AR frequency and intensity are also projected to increase along the AR tracks of the Southern Hemisphere's mid-to-high latitudes, with a slight expansion poleward[64]. However, future AR contribution to the Antarctic SMB is currently poorly constrained because the AR response to future climate change is highly dependent on the chosen detection tool[61,63] (Box 1), and algorithms use thresholds based on moisture fluxes, which are sensitive to increasing background moisture in a warmer climate. Studying future trends in blocking activities around Antarctica could offer important independent constraint on future AR changes[7,106]. Finally, introducing idealized aerosols with different residence times in atmospheric simulations and tracing polar aerosol ARs could help in disentangling the impact of the Clausius–Clapeyron effect from dynamic changes in future poleward transport and AR climatologies[48].

Overall, future changes in SMB could be somewhat offset by increases in solid ice discharge forced by the additional accumulation as proposed for the Amundsen Sea Embayment[107]. However, in the case of larger temperature increases, several ice shelves throughout Antarctica may even be at risk of collapse for this scenario owing to increased surface melt by the end of the twenty-first century[75,77,108–110].

Given the historical contributions of ARs to ice shelf surface melt and destabilization along the AP[10,36], as well as the role of AR-associated cyclones in ice shelf calving in other regions of Antarctica[79,80], it is likely that future ARs will function as key instigators of short-lived processes such as extreme surface melt and calving that affect the long-term stability and evolution of ice shelves, with heightened potential for ARs to trigger catastrophic ice shelf collapses in higher-end warming scenarios. Finally, although no studies have analysed future AR impacts on Antarctic sea ice, any future increases in AR frequency and/or intensity are likely to interact with the declining sea ice base state to increase the probability of extreme short-term sea ice loss events.

ARs have substantial impacts on surface variables across the Antarctic continent, driving extremes in precipitation, rainfall, temperature, melt and runoff. ARs are also associated with higher wind speeds and enhanced foehn events, impacting sea ice distribution and contributing to ocean swell, which may ultimately destabilize Antarctica's fragilized ice shelves. Although the future effects of ARs on ice sheet mass balance and local ecosystems remain poorly estimated, their role is expected to be critical, highlighting the need for future projections.

Summary and future perspectives

In this Review, we have established that ARs are a distinct extreme weather event connecting the global hydrometeorological cycle with AIS dynamics and ecosystems. Compared with other parts of the world, ARs around Antarctica have distinct global-scale dynamics related to lower latitude moisture export and eventual moisture deposition on the ice sheet. Over these southern polar regions, ARs have the ability to amplify the surrounding large-scale atmospheric circulation through their internal dynamics and latent heat release, further enhancing blocking conditions. The cold, dry atmosphere of the Antarctic means that detecting ARs requires polar-tuned detection algorithms using either relative or lower absolute thresholds for moisture transport compared with the mid-latitudes. These AR detection algorithms reveal that ARs are relatively rare occurrences around Antarctica, only occurring a few times per year at any given coastal location, but are a major driving force on regional precipitation trends and variability. Despite their rarity, ARs often have dramatic impacts on the AIS mass balance. At the present day, ARs have a positive influence on the mass balance through heavy snowfall. However, ARs can also cause coastal surface melting, sea ice erosion and ice shelf destabilization. These potential negative mass balance processes are expected to become more frequent in a warming climate. Warm airmass-related impacts are reflected in water stable isotope measurements, providing a possible avenue for studying past climate AR behaviour, in addition to disrupting the health of biological species across the continent. Observations of AR impacts on the AIS are sparse, but both past and future measurement campaigns hope to alleviate this data scarcity (Box 2).

Although substantial progress has been made in understanding the Antarctic AR life cycle and impacts, major research gaps persist. Starting with the life cycle of the AR-related moisture transport, ongoing research looks to uncover the various tropical forcing patterns necessary for the initial tropical moisture export and Rossby

wave amplification that directs that moisture towards Antarctica. This research includes systematically understanding the roles of the Madden Julian Oscillation and tropical cyclones while examining the stratosphere–tropopause link specifically regarding tropopause polar vortices. Once the moisture is transported over the AIS, questions remain over the influence this moisture exerts on mesoscale cyclonic activity. The use of high-resolution, kilometre-scale climate models can be useful in understanding how moisture transport within the warm conveyor belt influences cyclone intensity.

The uncertainties generated from polar AR detection techniques are also consequential to further understand AR impacts. Current methods of AR detection rely on tracing meridional moisture transport, which can neglect ARs affecting sea ice and the AP. Meanwhile, tracking ARs deeper into the AIS remains challenging because of the extremely low moisture threshold. Applying advances in AI-based image segmentation AR detection to the Antarctic could alleviate some of these issues[111,112]. As an alternative to detecting ARs via moisture transport, ARDTs can be designed to detect the poleward transport of other variables that can be found in narrow bands related to AR systems, such as aerosols and sensible and latent heat fluxes. These polar ARDTs have mostly been applied to reanalysis, which is relatively coarse in spatial resolution (for example, the Modern-Era Retrospective Analysis for Research and Applications Version 2, MERRA-2, reanalysis has a 0.5° latitude × 0.625° longitude spatial resolution, Box 1). Applying ARDTs to the next generation of kilometre-scale regional and global climate models could reveal greater detail on AR-related impacts, for example, the occurrence of rainfall in mountainous terrain[113].

Over Antarctica, major research gaps remain concerning AR impacts in the past, present and future. Further advanced targeted measurements of both AR characteristics and their impacts are required for process understanding and climate model evaluation. Detecting an AR signal within ice core records through water stable isotope analysis remains a priority, as it could enable climate reconstructions of Antarctic ARs before the reanalysis period (1979 onward). Likewise, determining the impacts of AR events of similar intensity as the March 2022 AR over the sensitive West Antarctic ice shelves is crucial for understanding extreme weather risks under sea-level rise projections. In addition, the simulation of ARs in future global climate model projections using polar-specific ARDTs will be important to uncover greater details about the magnitude of future increases in AR frequency and intensity and when ARs begin to be a net negative influence on AIS mass balance. One research gap identified during this Review was that Antarctic ARs are currently difficult to forecast. Given the precarious nature of Antarctic logistical operations, extreme weather events such as ARs can cause massive work interruptions and dangerous operating conditions. Thus, weather forecasting experiments envisioned from the Year of Polar Prediction – Southern Hemisphere 2022 targeted observing campaign are necessary to improve numerical weather prediction capabilities[114].

Understanding how short-lived weather extremes such as ARs can leave long-lasting (yearly–decadal–centennial) impacts on the AIS are only beginning to be recognized. Traditionally, projected changes in Antarctic mass balance have mostly been studied in relation to changes in mean climatology. However, as demonstrated in 2022, just a few extreme AR events can counteract the mean annual declining trend in ice mass balance. Yet, ARs are also capable of accelerating mass loss, as seen during the Larsen A and Larsen B ice shelf collapses in 1995 and 2002, respectively. The key question moving forward is how this balance between negative and positive impacts of ARs on the ice sheet mass balance will change with near-term and long-term climate change. Addressing this question in climate models will help to improve the understanding of how low-probability, high-impact events affect AIS instability and ultimately constrain future sea-level rise projections.

Data availability

ERA5 data produced by ECMWF are available through the Copernicus Climate Data Store (https://cds.climate.copernicus.eu/cdsapp#!/dataset/reanalysis-era5-pressure-levels?tab = overview). MERRA-2 data are publicly available at the Goddard Earth Sciences Data and Information Services Center (https://disc.gsfc.nasa.gov/datasets?project = MERRA-2). The code for the Wille et al. 2021 AR detection algorithm discussed in this study is publicly available (https://zenodo.org/record/7990215). Data for Fig. 2a are from ref. 7 and data for Fig. 2b are from ref. 49 with both data sets extended until 2020. The authors acknowledge use of imagery from the NASA Worldview application (https://worldview.earthdata.nasa.gov), part of the NASA Earth Observing System Data and Information System (EOSDIS), in Box 3.

Published online: 11 February 2025

References

1. Payne, A. E. et al. Responses and impacts of atmospheric rivers to climate change. *Nat. Rev. Earth Environ.* **1**, 143–157 (2020).
2. Nash, D., Waliser, D., Guan, B., Ye, H. & Ralph, F. M. The role of atmospheric rivers in extratropical and polar hydroclimate. *J. Geophys. Res. Atmos.* **123**, 6804–6821 (2018).
3. Zhu, Y. & Newell, R. E. A proposed algorithm for moisture fluxes from atmospheric rivers. *Mon. Weather Rev.* **126**, 725–735 (1998).
4. Turner, J. et al. The dominant role of extreme precipitation events in Antarctic snowfall variability. *Geophys. Res. Lett.* **46**, 3502–3511 (2019).
5. Morlighem, M. et al. Deep glacial troughs and stabilizing ridges unveiled beneath the margins of the Antarctic ice sheet. *Nat. Geosci.* **13**, 132–137 (2020).
6. Lemke, P. et al. in *Climate Change* 2007: *The Physical Science Basis — Contribution of Working Group I to the Fourth Assessment Report of the Intergovernmental Panel on Climate Change* Ch. 4 (Solomon, S. et al.) 337–383 (Cambridge Univ. Press, 2007).
7. Wille, J. D. et al. Antarctic atmospheric river climatology and precipitation impacts. *J. Geophys. Res. Atmos.* **126**, e2020JD033788 (2021).
8. Baiman, R., Winters, A. C., Lenaerts, J. & Shields, C. A. Synoptic drivers of atmospheric river induced precipitation near Dronning Maud Land, Antarctica. *J. Geophys. Res. Atmos.* **128**, e2022JD037859 (2023).
9. Baiman, R. et al. Synoptic and planetary-scale dynamics modulate antarctic atmospheric river precipitation intensity. *Commun. Earth Environ.* **5**, 127 (2024).
10. Wille, J. D. et al. West Antarctic surface melt triggered by atmospheric rivers. *Nat. Geosci.* **12**, 911–916 (2019).
11. Liang, K., Wang, J., Luo, H. & Yang, Q. The role of atmospheric rivers in Antarctic sea ice variations. *Geophys. Res. Lett.* **50**, e2022GL102588 (2023).
12. Gorodetskaya, I. V. et al. The role of atmospheric rivers in anomalous snow accumulation in East Antarctica. *Geophys. Res. Lett.* **41**, 6199–6206 (2014).
13. Boening, C., Lebsock, M., Landerer, F. & Stephens, G. Snowfall-driven mass change on the East Antarctic ice sheet. *Geophys. Res. Lett.* **39**, L21501 (2012).
14. Wille, J. D. et al. The extraordinary March 2022 East Antarctica 'Heat' wave. Part II: impacts on the Antarctic ice sheet. *J. Clim.* **37**, 779–799 (2024).
15. Francis, D., Mattingly, K. S., Temimi, M., Massom, R. & Heil, P. On the crucial role of atmospheric rivers in the two major Weddell Polynya events in 1973 and 2017 in Antarctica. *Sci. Adv.* **6**, eabc2695 (2020).
16. Bozkurt, D., Rondanelli, R., Marín, J. C. & Garreaud, R. Foehn event triggered by an atmospheric river underlies record-setting temperature along continental Antarctica. *J. Geophys. Res. Atmos.* **123**, 3871–3892 (2018).
17. Clem, K. R. et al. Antarctica and the Southern Ocean. *Bull. Am. Meteorol. Soc.* **104**, S322–S365 (2023).
18. Wang, Y., Wu, Q., Zhang, X. & Zhai, Z. Record-breaking Antarctic snowfall in 2022 delays global sea level rise. *Sci. Bull.* **68**, 3154–3157 (2023).
19. Pohl, B. et al. Relationship between weather regimes and atmospheric rivers in East Antarctica. *J. Geophys. Res. Atmos.* **126**, e2021JD035294 (2021).
20. Gorodetskaya, I. V. et al. Record-high Antarctic Peninsula temperatures and surface melt in February 2022: a compound event with an intense atmospheric river. *npj Clim. Atmos. Sci.* **6**, 202 (2023).
21. Spensberger, C., Reeder, M. J., Spengler, T. & Patterson, M. The connection between the southern annular mode and a feature-based perspective on Southern Hemisphere midlatitude winter variability. *J. Clim.* **33**, 115–129 (2020).

22. Goyal, R., Jucker, M., Sen Gupta, A., Hendon, H. H. & England, M. H. Zonal wave 3 pattern in the Southern Hemisphere generated by tropical convection. *Nat. Geosci.* **14**, 732–738 (2021).
23. Wille, J. D. et al. The extraordinary March 2022 East Antarctica 'Heat' wave. Part I: observations and meteorological drivers. *J. Clim.* **37**, 757–778 (2024).
24. Clem, K. R., Bozkurt, D., Kennett, D., King, J. C. & Turner, J. Central tropical Pacific convection drives extreme high temperatures and surface melt on the Larsen C Ice Shelf, Antarctic Peninsula. *Nat. Commun.* **13**, 3906 (2022).
25. Shields, C. A., Wille, J. D., Marquardt Collow, A. B., Maclennan, M. & Gorodetskaya, I. V. Evaluating uncertainty and modes of variability for Antarctic atmospheric rivers. *Geophys. Res. Lett.* **49**, e2022GL099577 (2022).
26. Terpstra, A., Gorodetskaya, I. V. & Sodemann, H. Linking sub-tropical evaporation and extreme precipitation over East Antarctica: an atmospheric river case study. *J. Geophys. Res. Atmos.* **126**, e2020JD033617 (2021).
27. Rondanelli, R., Hatchett, B., Rutllant, J., Bozkurt, D. & Garreaud, R. Strongest MJO on record triggers extreme Atacama rainfall and warmth in Antarctica. *Geophys. Res. Lett.* **46**, 3482–3491 (2019).
28. Trenberth, K. E. et al. Progress during TOGA in understanding and modeling global teleconnections associated with tropical sea surface temperatures. *J. Geophys. Res. Oceans* **103**, 14291–14324 (1998).
29. Wang, G. et al. Compounding tropical and stratospheric forcing of the record low Antarctic sea-ice in 2016. *Nat. Commun.* **10**, 13 (2019).
30. Wille, J. D. et al. Examining atmospheric river life cycles in East Antarctica. *J. Geophys. Res. Atmos.* **129**, e2023JD039970 (2024).
31. Maclennan, M. L. et al. Climatology and surface impacts of atmospheric rivers on West Antarctica. *Cryosphere* **17**, 865–881 (2023).
32. Gordon, A. E., Cavallo, S. M. & Novak, A. K. Evaluating common characteristics of Antarctic tropopause polar vortices. *J. Atmos. Sci.* **80**, 337–352 (2022).
33. Udy, D. G., Vance, T. R., Kiem, A. S., Holbrook, N. J. & Curran, M. A. J. Links between large-scale modes of climate variability and synoptic weather patterns in the Southern Indian Ocean. *J. Clim.* **34**, 883–899 (2021).
34. Bromwich, D. H. Snowfall in high southern latitudes. *Rev. Geophys.* **26**, 149 (1988).
35. Gehring, J. et al. Orographic flow influence on precipitation during an atmospheric river event at Davis, Antarctica. *J. Geophys. Res. Atmos.* **127**, e2021JD035210 (2022).
36. Wille, J. D. et al. Intense atmospheric rivers can weaken ice shelf stability at the Antarctic Peninsula. *Commun. Earth Environ.* **3**, 90 (2022).
37. Turner, J. et al. Extreme temperatures in the Antarctic. *J. Clim.* **34**, 2653–2668 (2021).
38. Datta, R. T. et al. The effect of Foehn-induced surface melt on firn evolution over the Northeast Antarctic Peninsula. *Geophys. Res. Lett.* **46**, 3822–3831 (2019).
39. Elvidge, A. D., Renfrew, I. A., King, J. C., Orr, A. & Lachlan-Cope, T. A. Foehn warming distributions in nonlinear and linear flow regimes: a focus on the Antarctic Peninsula: foehn warming distributions in nonlinear and linear flow regimes. *Q. J. R. Meteorol. Soc.* **142**, 618–631 (2016).
40. Zou, X. et al. Strong warming over the Antarctic Peninsula during combined atmospheric river and foehn events: contribution of shortwave radiation and turbulence. *J. Geophys. Res. Atmos.* **128**, e2022JD038138 (2023).
41. Laffin, M. K., Zender, C. S., van Wessem, M. & Marinsek, S. The role of föhn winds in eastern Antarctic Peninsula rapid ice shelf collapse. *Cryosphere* **16**, 1369–1381 (2022).
42. Elvidge, A. D., Kuipers Munneke, P., King, J. C., Renfrew, I. A. & Gilbert, E. Atmospheric drivers of melt on Larsen C Ice Shelf: surface energy budget regimes and the impact of foehn. *J. Geophys. Res. Atmos.* **125**, e2020JD032463 (2020).
43. Zou, X., Bromwich, D. H., Montenegro, A., Wang, S.-H. & Bai, L. Major surface melting over the Ross Ice Shelf part I: foehn effect. *Q. J. R. Meteorol. Soc.* **147**, 2874–2894 (2021).
44. Djoumna, G. & Holland, D. M. Atmospheric rivers, warm air intrusions, and surface radiation balance in the Amundsen Sea embayment. *J. Geophys. Res. Atmos.* **126**, e2020JD034119 (2021).
45. Francis, D., Fonseca, R., Mattingly, K. S., Lhermitte, S. & Walker, C. Foehn winds at Pine Island Glacier and their role in ice changes. *Cryosphere* **17**, 3041–3062 (2023).
46. Ricaud, P. et al. Supercooled liquid water cloud observed, analysed, and modelled at the top of the planetary boundary layer above Dome C, Antarctica. *Atmos. Chem. Phys.* **20**, 4167–4191 (2020).
47. Finlon, J. A. et al. Structure of an atmospheric river over Australia and the Southern Ocean: II. Microphysical evolution. *J. Geophys. Res. Atmos.* **125**, e2020JD032514 (2020).
48. Lapere, R. et al. Polar aerosol atmospheric rivers: detection, characteristics, and potential applications. *J. Geophys. Res. Atmos.* **129**, e2023JD039606 (2024).
49. Maclennan, M. L., Lenaerts, J. T. M., Shields, C. & Wille, J. D. Contribution of atmospheric rivers to Antarctic precipitation. *Geophys. Res. Lett.* **49**, e2022GL100585 (2022).
50. Zhang, Z. et al. Extending the CW3E atmospheric river scale to the polar regions. *EGUsphere* **2024**, 1–36 (2024).
51. Marshall, G. J. & Thompson, D. W. J. The signatures of large-scale patterns of atmospheric variability in Antarctic surface temperatures: Antarctic temperatures. *J. Geophys. Res. Atmos.* **121**, 3276–3289 (2016).
52. Clem, K. R., Renwick, J. A., McGregor, J. & Fogt, R. L. The relative influence of ENSO and SAM on Antarctic Peninsula climate. *J. Geophys. Res. Atmos.* **121**, 9324–9341 (2016).
53. Nuncio, M. & Yuan, X. The influence of the Indian Ocean dipole on Antarctic sea ice. *J. Clim.* **28**, 2682–2690 (2015).
54. Fogt, R. L. et al. Seasonal Antarctic pressure variability during the twentieth century from spatially complete reconstructions and CAM5 simulations. *Clim. Dyn.* **53**, 1435–1452 (2019).
55. Turner, J. et al. Antarctic temperature variability and change from station data. *Int. J. Climatol.* **40**, 2986–3007 (2020).
56. Maclennan, M. L. & Lenaerts, J. T. M. Large-scale atmospheric drivers of snowfall over Thwaites Glacier, Antarctica. *Geophys. Res. Lett.* **48**, e2021GL093644 (2021).
57. Zhang, N., Zheng, X. & Ma, Q. Study on wave-induced kinematic responses and flexures of ice floe by smoothed particle hydrodynamics. *Comput. Fluids* **189**, 46–59 (2019).
58. Guo, Y., Shinoda, T., Guan, B., Waliser, D. E. & Chang, E. K. M. Statistical relationship between atmospheric rivers and extratropical cyclones and anticyclones. *J. Clim.* **33**, 7817–7834 (2020).
59. Zhang, Z. & Ralph, F. M. The influence of antecedent atmospheric river conditions on extratropical cyclogenesis. *Mon. Weather Rev.* **149**, 1337–1357 (2021).
60. Ma, W., Chen, G. & Guan, B. Poleward shift of atmospheric rivers in the Southern Hemisphere in recent decades. *Geophys. Res. Lett.* **47**, e2020GL089934 (2020).
61. Shields, C. A. et al. Future atmospheric rivers and impacts on precipitation: overview of the ARTMIP Tier 2 high-resolution global warming experiment. *Geophys. Res. Lett.* **50**, e2022GL102091 (2023).
62. Ma, W. et al. The role of interdecadal climate oscillations in driving Arctic atmospheric river trends. *Nat. Commun.* **15**, 2135 (2024).
63. O'Brien, T. A. et al. Increases in future AR count and size: overview of the ARTMIP Tier 2 CMIP5/6 experiment. *J. Geophys. Res. Atmos.* **127**, e2021JD036013 (2022).
64. Zhang, L., Zhao, Y., Cheng, T. F. & Lu, M. Future changes in global atmospheric rivers projected by CMIP6 models. *J. Geophys. Res. Atmos.* **129**, e2023JD039359 (2024).
65. Otosaka, I. N. et al. Mass balance of the Greenland and Antarctic ice sheets from 1992 to 2020. *Earth Syst. Sci. Data* **15**, 1597–1616 (2023).
66. Mottram, R. et al. What is the surface mass balance of Antarctica? An intercomparison of regional climate model estimates. *Cryosphere* **15**, 3751–3784 (2021).
67. Lenaerts, J. T. M., Medley, B., van den Broeke, M. R. & Wouters, B. Observing and modeling ice sheet surface mass balance. *Rev. Geophys.* **57**, 376–420 (2019).
68. Rignot, E. et al. Four decades of Antarctic Ice Sheet mass balance from 1979–2017. *Proc. Natl Acad. Sci. USA* **116**, 1095 (2019).
69. González-Herrero, S. et al. Extreme precipitation records in Antarctica. *Int. J. Climatol.* **43**, 3125–3138 (2023).
70. Adusumilli, S., Fish, A. M., Fricker, H. A. & Medley, B. Atmospheric river precipitation contributed to rapid increases in surface height of the West Antarctic Ice Sheet in 2019. *Geophys. Res. Lett.* **48**, e2020GL091076 (2021).
71. Evangelista, H. et al. The June 2022 extreme warm event in central West Antarctica. *Antarctic Sci.* **35**, 319–327 (2023).
72. Bozkurt, D., Marín, J. C. & Barrett, B. S. Temperature and moisture transport during atmospheric blocking patterns around the Antarctic Peninsula. *Weather Clim. Extrem.* **38**, 100506 (2022).
73. Amory, C. et al. Firn on ice sheets. *Nat. Rev. Earth Environ.* **5**, 79–99 (2024).
74. Kuipers Munneke, P., Ligtenberg, S. R. M., Van Den Broeke, M. R. & Vaughan, D. G. Firn air depletion as a precursor of Antarctic ice-shelf collapse. *J. Glaciol.* **60**, 205–214 (2014).
75. Donat-Magnin, M. et al. Future surface mass balance and surface melt in the Amundsen sector of the West Antarctic Ice Sheet. *Cryosphere* **15**, 571–593 (2021).
76. Van Wessem, J. M., Van De Berg, W. J. & Van Den Broeke, M. R. Data set: monthly averaged RACMO2.3p2 variables; Antarctica. *Zenodo* https://doi.org/10.5281/zenodo.7845736 (2023).
77. Gilbert, E. & Kittel, C. Surface melt and runoff on Antarctic ice shelves at 1.5 °C, 2 °C, and 4 °C of future warming. *Geophys. Res. Lett.* **48**, e2020GL091733 (2021).
78. Scambos, T., Hulbe, C. & Fahnestock, M. Climate-induced ice shelf disintegration in the Antarctic Peninsula. in *Antarctic Peninsula Climate Variability*: *Historical and Paleoenvironmental Perspectives* (eds Domack, E. et al.) 79–92 (Wiley, 2003).
79. Francis, D., Mattingly, K. S., Lhermitte, S., Temimi, M. & Heil, P. Atmospheric extremes caused high oceanward sea surface slope triggering the biggest calving event in more than 50 years at the Amery Ice Shelf. *Cryosphere* **15**, 2147–2165 (2021).
80. Francis, D. et al. Atmospheric triggers of the Brunt Ice Shelf calving in February 2021. *J. Geophys. Res. Atmos.* **127**, e2021JD036424 (2022).
81. Walker, C. C. et al. Multi-decadal collapse of East Antarctica's Conger–Glenzer Ice Shelf. *Nat. Geosci.* **17**, 1240–1248 (2024).
82. Ochwat, N. E. et al. Triggers of the 2022 Larsen B multi-year landfast sea ice breakout and initial glacier response. *Cryosphere* **18**, 1709–1731 (2024).
83. Stammerjohn, S. et al. Antarctica and the Southern Ocean. *Bull. Am. Meteorol. Soc.* **102**, S317–S356 (2021).
84. Kuipers Munneke, P. et al. Intense winter surface melt on an Antarctic Ice Shelf. *Geophys. Res. Lett.* **45**, 7615–7623 (2018).
85. Hepworth, E., Messori, G. & Vichi, M. Association between extreme atmospheric anomalies over Antarctic sea ice, Southern Ocean Polar cyclones and atmospheric rivers. *J. Geophys. Res. Atmos.* **127**, e2021JD036121 (2022).
86. Bozkurt, D. et al. Recent near-surface temperature trends in the Antarctic Peninsula from observed, reanalysis and regional climate model data. *Adv. Atmos. Sci.* **37**, 477–493 (2020).

87. Fonseca, R. et al. Atmospheric controls on the Terra Nova Bay polynya occurrence in Antarctica. *Clim. Dyn.* **61**, 5147–5169 (2023).
88. Jena, B. et al. Record low sea ice extent in the Weddell Sea, Antarctica in April/May 2019 driven by intense and explosive polar cyclones. *npj Clim. Atmos. Sci.* **5**, 19 (2022).
89. Kriegsmann, A. & Brümmer, B. Cyclone impact on sea ice in the central Arctic Ocean: a statistical study. *Cryosphere* **8**, 303–317 (2014).
90. Holland, P. R. & Kimura, N. Observed concentration budgets of Arctic and Antarctic sea ice. *J. Clim.* **29**, 5241–5249 (2016).
91. Massom, R. A. et al. Antarctic ice shelf disintegration triggered by sea ice loss and ocean swell. *Nature* **558**, 383–389 (2018).
92. Raphael, M. N. & Handcock, M. S. A new record minimum for Antarctic sea ice. *Nat. Rev. Earth Environ.* **3**, 215–216 (2022).
93. Lu, H. et al. Extreme warm events in the South Orkney Islands, Southern Ocean: compounding influence of atmospheric rivers and föhn conditions. *Q. J. R. Meteorol. Soc.* **149**, 3645–3668 (2023).
94. Torres, C., Bozkurt, D., Carrasco-Escaff, T., Bolibar, J. & Arigony-Neto, J. New insights on the interannual surface mass balance variability on the South Shetland Islands glaciers, northerly Antarctic Peninsula. *Glob. Planet. Change* **239**, 104506 (2024).
95. Ropert-Coudert, Y. et al. A complete breeding failure in an Adélie penguin colony correlates with unusual and extreme environmental events. *Ecography* **38**, 111–113 (2015).
96. Barrett, J. E. et al. Response of a terrestrial polar ecosystem to the March 2022 Antarctic weather anomaly. *Earths Future* **12**, e2023EF004306 (2024).
97. Jackson, S. L. et al. Climatology of the Mount Brown South ice core site in East Antarctica: implications for the interpretation of a water isotope record. *Clim. Past* **19**, 1653–1675 (2023).
98. Weng, Y., Johannessen, A. & Sodemann, H. High-resolution stable isotope signature of a land-falling atmospheric river in southern Norway. *Weather Clim. Dyn.* **2**, 713–737 (2021).
99. Bozkurt, D. et al. Atmospheric river brings warmth and rainfall to the Northern Antarctic Peninsula during the mid-Austral Winter of 2023. *Geophys. Res. Lett.* **51**, e2024GL108391 (2024).
100. Hoffmann-Abdi, K. et al. Short-term meteorological and environmental signals recorded in a firn core from a high-accumulation site on Plateau Laclavere, Antarctic Peninsula. *Geosciences* **11**, 428 (2021).
101. Favier, V. et al. Antarctica-regional climate and surface mass budget. *Curr. Clim. Change Rep.* **3**, 303–315 (2017).
102. Kittel, C. et al. Diverging future surface mass balance between the Antarctic ice shelves and grounded ice sheet. *Cryosphere* **15**, 1215–1236 (2021).
103. Coulon, V. et al. Disentangling the drivers of future Antarctic ice loss with a historically calibrated ice-sheet model. *Cryosphere* **18**, 653–681 (2024).
104. Dalaiden, Q. et al. How useful is snow accumulation in reconstructing surface air temperature in Antarctica? A study combining ice core records and climate models. *Cryosphere* **14**, 1187–1207 (2020).
105. Vignon, É., Roussel, M.-L., Gorodetskaya, I. V., Genthon, C. & Berne, A. Present and future of rainfall in Antarctica. *Geophys. Res. Lett.* **48**, e2020GL092281 (2021).
106. Scott, R. C., Nicolas, J. P., Bromwich, D. H., Norris, J. R. & Lubin, D. Meteorological drivers and large-scale climate forcing of West Antarctic surface melt. *J. Clim.* **32**, 665–684 (2019).
107. Bevan, S. et al. Amundsen Sea embayment ice-sheet mass-loss predictions to 2050 calibrated using observations of velocity and elevation change. *J. Glaciol.* **69**, 1729–1739 (2023).
108. Trusel, L. D. et al. Divergent trajectories of Antarctic surface melt under two twenty-first-century climate scenarios. *Nat. Geosci.* **8**, 927–932 (2015).
109. Lowry, D. P., Krapp, M., Golledge, N. R. & Alevropoulos-Borrill, A. The influence of emissions scenarios on future Antarctic ice loss is unlikely to emerge this century. *Commun. Earth Environ.* **2**, 221 (2021).
110. Lai, C.-Y. et al. Vulnerability of Antarctica's ice shelves to meltwater-driven fracture. *Nature* **584**, 574–578 (2020).
111. Mahesh, A. et al. Identifying atmospheric rivers and their poleward latent heat transport with generalizable neural networks: ARCNNv1. *Geosci. Model Dev.* **17**, 3533–3557 (2024).
112. Galea, D., Ma, H.-Y., Wu, W.-Y. & Kobayashi, D. Deep learning image segmentation for atmospheric rivers. *Artif. Intell. Earth Syst.* **3**, 230048 (2024).
113. Gilbert, E. et al. Extreme precipitation associated with atmospheric rivers over West Antarctic ice shelves: insights from kilometre-scale regional climate modelling. *EGUsphere* **2024**, 1–41 (2024).
114. Bromwich, D. H. et al. Winter targeted observing periods during the Year of Polar Prediction in the Southern Hemisphere (YOPP-SH). *Bull. Am. Meteorol. Soc.* **105**, E1662–E1684 (2024).
115. Gelaro, R. et al. The modern-era retrospective analysis for research and applications, version 2 (MERRA-2). *J. Clim.* **30**, 5419–5454 (2017).
116. Shields, C. A. et al. Atmospheric River Tracking Method Intercomparison Project (ARTMIP): project goals and experimental design. *Geosci. Model Dev.* **11**, 2455–2474 (2018).
117. Rutz, J. J. et al. The Atmospheric River Tracking Method Intercomparison Project (ARTMIP): quantifying uncertainties in atmospheric river climatology. *J. Geophys. Res. Atmos.* **124**, 13777–13802 (2019).
118. Gorodetskaya, I. V., Silva, T., Schmithüsen, H. & Hirasawa, N. Atmospheric river signatures in radiosonde profiles and reanalyses at the Dronning Maud Land Coast, East Antarctica. *Adv. Atmos. Sci.* **37**, 455–476 (2020).
119. Hersbach, H. et al. The ERA5 global reanalysis. *Q. J. R. Meteorol. Soc.* **146**, 1999–2049 (2020).
120. Ralph, F. M. et al. A scale to characterize the strength and impacts of atmospheric rivers. *Bull. Am. Meteorol. Soc.* **100**, 269–289 (2019).
121. Ricaud, P. et al. Supercooled liquid water clouds observed over Dome C, Antarctica: temperature sensitivity and cloud radiative forcing. *Atmos. Chem. Phys.* **24**, 613–630 (2024).
122. Mitnik, L. M., Kuleshov, V. P., Mitnik, M. L. & Baranyuk, A. V. Satellite microwave radiometric measurements of extreme temperature rise in East Antarctica in March 2022. *Sovr. Probl. DZZ Kosm.* **20**, 246–261 (2023).
123. Crewell, S. et al. A systematic assessment of water vapor products in the Arctic: from instantaneous measurements to monthly means. *Atmos. Meas. Tech.* **14**, 4829–4856 (2021).
124. Hoffman, A. O., Maclennan, M., Lenaerts, J., Larson, K. M. & Chrsitianson, K. Amundsen Sea embayment accumulation variability measured with GNSS-IR. *Cryosphere Discuss.* **2023**, 1–28 (2023).
125. Bromwich, D. H. et al. The Year of Polar Prediction in the Southern Hemisphere (YOPP-SH). *Bull. Am. Meteorol. Soc.* **101**, E1653–E1676 (2020).
126. Culberg, R., Schroeder, D. M. & Chu, W. Extreme melt season ice layers reduce firn permeability across Greenland. *Nat. Commun.* **12**, 2336 (2021).
127. Miller, J. Z. et al. An empirical algorithm to map perennial firn aquifers and ice slabs within the Greenland Ice Sheet using satellite L-band microwave radiometry. *Cryosphere* **16**, 103–125 (2022).
128. Neff, P. Amundsen Sea coastal ice rises: future sites for marine-focused ice core records. *Oceanography* **33**, 88–89 (2020).
129. Graf, P., Wernli, H., Pfahl, S. & Sodemann, H. A new interpretative framework for below-cloud effects on stable water isotopes in vapour and rain. *Atmos. Chem. Phys.* **19**, 747–765 (2019).
130. Fauchereau, N., Pohl, B., Reason, C. J. C., Rouault, M. & Richard, Y. Recurrent daily OLR patterns in the Southern Africa/Southwest Indian Ocean region, implications for South African rainfall and teleconnections. *Clim. Dyn.* **32**, 575–591 (2009).
131. Pohl, B., Dieppois, B., Crétat, J., Lawler, D. & Rouault, M. From synoptic to interdecadal variability in Southern African rainfall: toward a unified view across time scales. *J. Clim.* **31**, 5845–5872 (2018).
132. Hart, N. C. G., Reason, C. J. C. & Fauchereau, N. Cloud bands over southern Africa: seasonality, contribution to rainfall variability and modulation by the MJO. *Clim. Dyn.* **41**, 1199–1212 (2013).
133. Macron, C., Pohl, B., Richard, Y. & Bessafi, M. How do tropical temperate troughs form and develop over Southern Africa? *J. Clim.* **27**, 1633–1647 (2014).
134. Wernli, H. A Lagrangian-based analysis of extratropical cyclones. II: A detailed case-study. *Q. J. R. Meteorol. Soc.* **123**, 1677–1706 (1997).
135. Servettaz, A. P. M. et al. Snowfall and water stable isotope variability in East Antarctica controlled by warm synoptic events. *J. Geophys. Res. Atmos.* **125**, e2020JD032863 (2020).

Acknowledgements

J.D.W. acknowledges support from the Horizon 2020 project nextGEMS under grant agreement number 101003470. K.S.M. acknowledges support from the Polar Radiant Energy in the Far InfraRed Experiment (PREFIRE) mission, NASA grant 80NSSC18K1485. X.Z. acknowledges support from NSF Grants 2229392. Y.M. was supported by the NASA Future Investigators in NASA Earth and Space Science and Technology programme (award number 80NSSC24K0012). J.E.B. was supported by the National Science Foundation for Long Term Ecological Research number OPP-2224760. C.A.S. acknowledges support by the Regional and Global Model Analysis (RGMA) component of the Earth and Environmental System Modeling Program of the US Department of Energy's Office of Biological & Environmental Research (BER) under Award Number DE-SC0022070, as well as National Center for Atmospheric Research, sponsored by NSF, under Cooperative Agreement Number 1852977. K.R.C. acknowledges support from the Royal Society of New Zealand Marsden Fund grant MFP-VUW2010. G.L. was supported by the National Defense Science and Engineering Graduate (NDSEG) Fellowship programme. A.C.W. and R.B. acknowledge financial support from the University of Colorado Boulder. M.L.M. acknowledges support from NASA grant 80NSSC21K1610 and the University of Colorado Boulder. I.V.G. thanks the support by the strategic funding to CIIMAR (UIDB/04423/2020 and UIDP/04423/2020), 2021.03140. CEECIND, projects ATLACE (CIRCNA/CAC/0273/2019), MAPS (2022.09201.PTDC) and Portuguese Polar Program (PROPOLAR) through national funds provided by FCT (Fundação para a Ciência e a Tecnologia). D.B. acknowledges support from ANID-FONDECYT-1240190, ANID-FONDAP-1523A0002 and COPAS COASTAL ANID FB210021. A.C. and S.K. acknowledge funding support from the Ukrainian State Special-Purpose Research Program in Antarctica for 2011–2022, research direction: Hydrometeorology; and they express their gratitude to their Ukrainian polar science co-workers known as the 'Squad of Combat Penguins'.

Author contributions

J.D.W., V.F. and I.V.G. led the Review. All authors contributed to the researching of data, writing and reviewing and editing of the manuscript, with authors B.P., R.B., I.V.G., C.A.S., M.L.M., X.Z., D.B., V.F., J.D.W. and R.D. leading the contributions to specific sections. Figure and display items were led by the following authors: B.P. (Fig. 1), R.B. (Figs. 1 and 2), X.Z. (Figs. 1 and 3), A.O.H. (Fig. 4), I.V.G. (Boxes 1 and 2) and V.F. and J.D.W. (Box 3).

Competing interests

C.A.S. is an associate editor for *NPJ Climate and Atmospheric Science*. The other authors declare no competing interests.

Additional information
Peer review information *Nature Reviews Earth & Environment* thanks Sergi González-Herrero, Qinghua Yang, Ella Gilbert and the other, anonymous, reviewer(s) for their contribution to the peer review of this work.

[1]Institute for Atmospheric and Climate Science, ETH Zurich, Zurich, Switzerland. [2]Institut des Géosciences de l'Environnement, CNRS/UGA/IRD/G-INP, Saint Martin d'Hères, France. [3]CIIMAR, Interdisciplinary Centre of Marine and Environmental Research, University of Porto, Porto, Portugal. [4]Laboratoire des Sciences du Climat et de l'Environnement, UMR 8212 CEA-CNRS-UVSQ, Université Paris-Saclay, IPSL, Gif-sur-Yvette, France. [5]Department of Atmospheric and Oceanic Sciences, University of Colorado Boulder, Boulder, CO, USA. [6]Department of Biological Sciences, Virginia Tech, Blacksburg, VA, USA. [7]Laboratoire d'Océanographie et du Climat, LOCEAN-IPSL, Sorbonne Université, CNRS, IRD, MNHN, Paris, France. [8]Eurasia Institute of Earth Sciences, Istanbul Technical University, Istanbul, Turkey. [9]Department of Meteorology, University of Valparaíso, Valparaíso, Chile. [10]Center for Climate and Resilience Research (CR)2, Santiago, Chile. [11]Center for Oceanographic Research COPAS COASTAL, University of Concepción, Concepción, Chile. [12]Ukrainian Hydrometeorological Institute, Kyiv, Ukraine. [13]National Antarctic Scientific Center of Ukraine, Kyiv, Ukraine. [14]School of Geography, Environment and Earth Sciences, Victoria University of Wellington, Wellington, New Zealand. [15]Department of Geoscience and Remote Sensing, Delft University of Technology, Delft, Netherlands. [16]Environmental and Geophysical Sciences (ENGEOS) Lab, Khalifa University of Science and Technology, Abu Dhabi, United Arab Emirates. [17]Lamont-Doherty Earth Observatory, Columbia University, Palisades, NY, USA. [18]Faculty of Science and Engineering, University of Groningen, Groningen, Netherlands. [19]Department of Atmospheric and Ocean Sciences, University of Maryland, College Park, MD, USA. [20]Space Science and Engineering Center, University of Wisconsin — Madison, Madison, WI, USA. [21]Department of Geography, University of California Santa Barbara, Santa Barbara, CA, USA. [22]Biogéosciences, CNRS/Université Bourgogne Europe, Dijon, France. [23]Climate and Global Dynamics Lab, NSF National Center for Atmospheric Research, Boulder, CO, USA. [24]CW3E, Scripps Institution of Oceanography, University of California San Diego, San Diego, CA, USA. [25]Cooperative Institute for Research in Environmental Sciences, University of Colorado Boulder, Boulder, CO, USA. [26]These authors contributed equally: Jonathan D. Wille, Vincent Favier, Irina V. Gorodetskaya.